IEEE Access
Multidisciplinary | Rapid Review | Open Access Journal

Received September 3, 2019, accepted September 9, 2019, date of publication September 17, 2019, date of current version October 8, 2019.

Digital Object Identifier 10.1109/ACCESS.2019.2941965

Influence of Sintering Temperature and ZrO_2 Dopants on the Microstructure and Electrical Properties of Zinc Oxide Varistors

PENGKANG XIE AND JIANPING HU

State Key Laboratory of Disaster Prevention and Reduction for Power Grid Transmission and Distribution Equipment, Changsha 410007, China

Corresponding author: Pengkang Xie (xiepengkang@126.com)

This work was supported in part by the Changsha Science and Technology Project in Hunan Province under Grant kq 1804051, and in part by the Science and Technology Project of State Grid Corporation of China under Grant 5216A01600W3 and Grant 5216A01800JG.

ABSTRACT This paper investigated the effects of sintering temperature on the microstructure and electrical properties of ZrO_2-doped zinc oxide (ZnO) varistor ceramics. The results show that, the additive ZrO_2 exists as independent second phase between ZnO grains, which can limit the growth of ZnO grains and improve the voltage gradient. With the increasing of ZrO_2, the content of extrinsic elements (Mn, Sb, Co, Cr) in the grain boundary layers tends to increase first and then decease. When ZrO_2 content is more than 1.0mol%, the electrical performance of ZnO varistors decreases sharply. With the increasing of sintering temperature, the ZnO grain size increases and the voltage gradient decreases. When the sintering temperature is larger than 1200°C, more monoclinic ZrO_2 phase transformed into cubic phase, and more micropores are generated, causing the non-linear coefficient to decrease and the residual voltage ratio and leakage current to increase. With a sintering temperature of 1150°C and a ZrO_2 content of 1.0mol%, the ZnO varistors can reach the overall optimum electric performance, exhibiting a breakdown voltage of $E_{1mA} = 420$V/mm, a nonlinear coefficient of $\alpha = 58$, a residual voltage ratio of $C_R = 1.87$, and a leakage current of $I_L = 4\mu$A. The studies in this paper can give reference for the development of high quality ZnO arresters.

INDEX TERMS Varistors, temperature control, ceramics.

I. INTRODUCTION

Because of the excellent nonlinear V-I characteristics and energy absorption capability, metal oxide arresters (MOAs) are widely used in power systems to protect electric equipments from transient over-voltages [1]–[5]. ZnO varistors, which are the core components of MOAs, can be made by mixing and sintering ZnO powder with other minor oxide additives, such as Co_2O_3, MnO_2, Bi_2O_3, Sb_2O_3, Cr_2O_3 and so on [6]–[14]. As MOAs used in high voltage power systems are usually very long, in order to meet the requirements to save space in high voltage power systems, high gradient ZnO varistors are needed [2], [4], [15]–[18]. At the same time, nonlinear coefficient and residual voltage ratio of the ZnO varistors can affect the insulation co-ordination design of high voltage power systems, and it is necessary to develop ZnO varistors with a high nonlinear coefficient and a low residual voltage ratio [10]–[13], [15], [19]. In addition, leakage current is also an important parameter of ZnO varistors, which has a great influence on the service life of MOAs [17], [20]–[23]. Thus, it is of great significance to improve the voltage gradient of ZnO varistors with a small leakage current, a high non-linear coefficient and a low residual voltage ratio.

In most industrial applications, ZnO varistors are manufactured by sintering the mixture of ZnO powder and traces of metal oxide additives at a temperature from 1000°C to 1300°C [24]–[27]. In previous studies, it has been proved that the electric characteristics of ZnO varistors are determined by their microstructures, which can be effectively improved by the introduction of metal oxides [28], [29]. Additive metal oxides such as Cr_2O_3, Co_2O_3 and MnO_2 can be used to provide ions and form interstitial states, which ultimately leads to the improvement of potential barrier [30]–[32]. The influence of Sb_2O_3, TiO_2, BaO, SiO_2, Y_2O_3 and Cr_2O_3 was studied, and these additives have been proved to be

The associate editor coordinating the review of this manuscript and approving it for publication was Mahmoud Al Ahmad.

effectively in improving the electric characteristics of ZnO varistors [33]–[37]. Exist studies in [33] found that ZrO_2 can improve the voltage gradient of ZnO varistors, but till now, little work has been done to study the effects of ZrO_2 addictives on the element distribution, crystal phase and electric characteristics of ZnO varistors. It has been reported that sintering temperature can effectively influence the electric characteristics and microstructure of ZnO varistors [13], [2], [17], [18], but little has been done to study the combined effects of sintering temperature and ZrO_2 addictives.

In view of the above, in order to improve the electric characteristics of ZnO varistors, this paper studied the combined effects of ZrO_2 dopants and sintering temperature on the microstructure and electrical properties of ZnO varistors. X-ray diffraction (XRD) and scanning electron microscope (SEM) coupled with energy dispersive spectrometer (EDS) have been applied to study the phase evolution and microstructure of the ZrO_2-doped varistors. Bulk density of the samples was measured, the V-I characteristics, breakdown voltage, residual voltage ratio as well as leakage current of the manufactured ZnO varistors were obtained. Impedance measurement was done to obtain the resistance of ZnO grains and grain boundary layers. The experimental results were analyzed and discussed, based on which suggested ZrO_2 content and sintering temperature have been given to obtain the optimum electric characteristics.

II. EXPERIMENTAL

A. SAMPLE PREPARATION

Solid-state reaction method was adopted to manufacture the ZnO varistors, and the compositions are as follow: (94.85-x) mol% ZnO, 0.6mol% Bi_2O_3, 0.59mol% MnO_2, 1.0mol% Co_2O_3, 0.34mol% Cr_2O_3, 1mol% Sb_2O_3, 1.47mol% SiO_2, 0.15mol% $Al(NO)_3{\cdot}9H_2O$ and x mol% ZrO_2(x = 0.0, 0.2, 0.5, 1.0, 1.5, and 2.0). Reagent-grade raw materials were used, the powders were firstly mixed in specific proportion with deionized water, then the mixed sizing agent was subjected to high energy ball milling for 30min. After milling, spraying granulating process was applied and the mixed powder was pressed at discs of 40mm diameter and 20mm thickness [17]. The density of the pressed discs was 3.2g/cm^3. The samples were then sintered at temperatures from 1000°C to 1250°C for 6h in a furnace (Daheng SG-XL1400, Shanghai). The heating rate is 1.5°C/min and the cooling rate is 2.5°C/min. When the sintering temperature is cooled to room temperature, an aluminum electrode was finally coated on the surface of the samples.

B. CHARACTERIZATION

In order to indentify the crystal phase of the prepared samples, XRD analysis (8000 S/L, State Grid Corp, German) has been applied for identification. SEM (XU3010, Leiyu, Japan) was used for microstructure observations. The element content in different parts of the crystal phases were identified using energy dispersive spectrometer (EDS, XMAX 70, Texas Instruments, Japan).

The V-I curves of the samples in the small current region have been obtained using an AC voltage-current meter in State Grid Hunan corporation. The breakdown voltage per millimeter (E_{1mA}) was measured at the current of 1.0mA, and the leakage current (I_L) was obtained at 75% of the breakdown voltage. E_{1mA} and I_L were obtained using voltage generator and current meter(10xbc, Huatian, China). The nonlinear coefficient (α) can be calculated as follow: [2], [16], [17]

$$\alpha = \frac{\log J_2 - \log J_1}{\log E_2 - \log E_1} \tag{1}$$

In Equation (1), J_1 and J_2 mean current densities. J_1 is chosen as 0.1mA/cm^2 and J_2 equals 1mA/cm^2. E_1 and E_2 are the electric fields of the ZnO varistors corresponding to J_1 and J_2. Impulse currents with a magnitude of 5kA and a waveform of 4/10μs were applied to the prepared samples, the residual voltage was measured and residual voltage ratio (C_R) was calculated.

The resistance of ZnO grain and grain boundary was obtained using impedance analyzer. According to the electric model of ZnO varistors in [2], [4], [10], [15]–[18], the resistance of ZnO grain is much smaller than grain boundary, and the grain boundary resistance can be measured when the applied frequency is 0, and the ZnO grain resistance was measured when the applied frequency is 13MHz [9]–[13].

III. RESULTS AND DISCUSSION

A. MICROSTRUCTURE AND XRD OBSERVATION

Fig. 1 shows the X-ray diffraction spectrums of the manufactured ZnO varistors. The results show the presence of ZnO phase and minor phase of Bi_2O_3, Zn_2SiO_4 and $Zn_{2.33}Sb_{0.67}O_4$. Independent monoclinic and cubic phases of ZrO_2 can also be observed. The XRD patterns of the tested samples in Fig. 1 show little phase shifts with different ZrO_2 contents.

According to Fig.1, using MDI Jade software, the crystal structure can be obtained [15]. The sintering temperature and

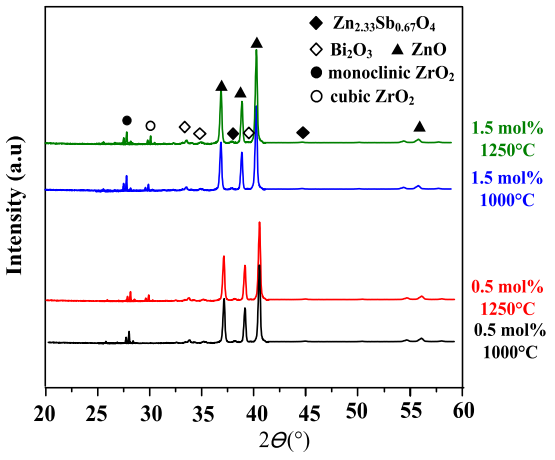

FIGURE 1. XRD patterns of ZnO varistors with various sintering temperatures and ZrO_2 additives.

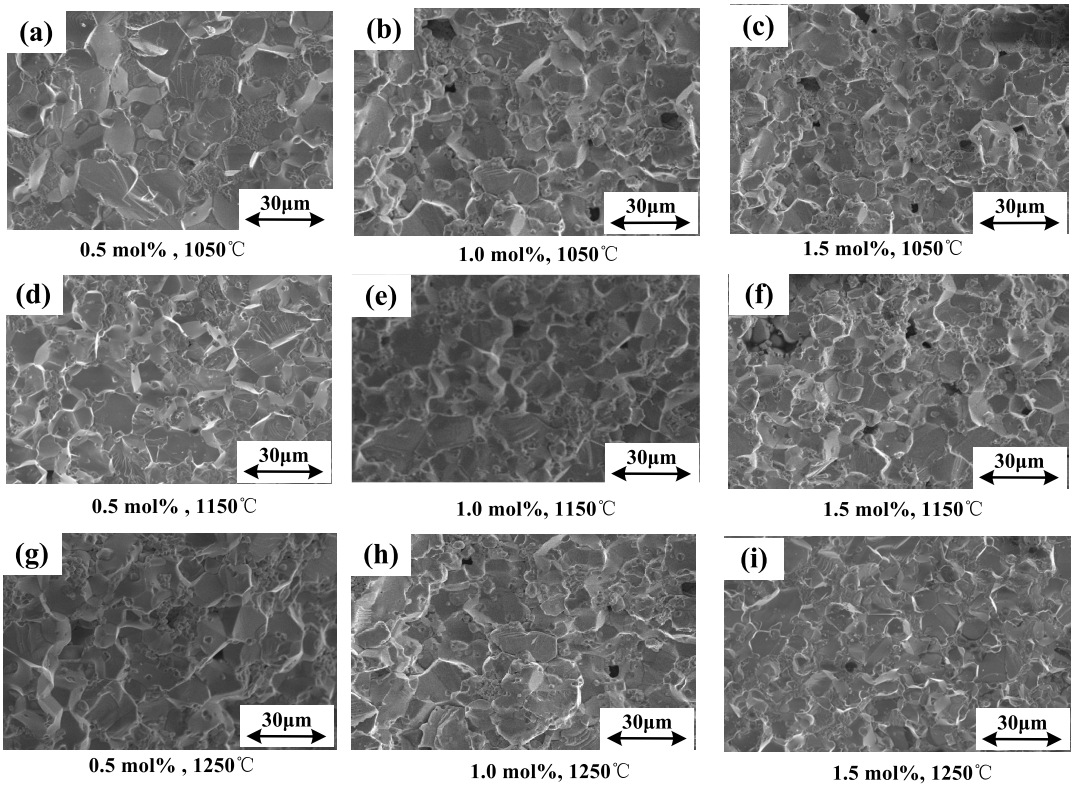

FIGURE 2. SEM micrographs ZnO of samples with different ZrO2 contents and sintering at different temperatures.

TABLE 1. The diffracted intensity of ZrO_2 phase with different ZrO_2 content and sintering temperature.

	Diffracted intensity(a.u)			
	0.5mol% 1000℃	0.5mol% 1200℃	1.5mol% 1000℃	1.5mol% 1200℃
Monoclinic phase	0.057	0.045	0.173	0.137
Cubic phase	0.01	0.022	0.028	0.065

additive ZrO_2 content influence little on the crystal structure of hexagonal ZnO phase, the lattice parameters of ZnO are: a=b=3.24Å, c = 5.19Å, $\beta = 90°$. The cell volume is 1.42×10^{-28}m. The additive ZrO_2 exists as independent second phase and do not reacted with or dissolved into ZnO grains during the sintering process. The lattice parameters of cubic ZrO_2 phase are: a=b=c=5.2Å, $\beta = 99°$, the cell volume is 1.39×10^{-28}m. The lattice parameters of monoclinic ZrO_2 phase are: a=b=c=5.1Å, $\beta = 90°$, the cell volume is 1.33×10^{-28}m.

Assuming the diffraction intensity of ZnO to be 1 a.u, the diffracted intensity variation of different ZrO_2 phase with additive ZrO_2 content and sintering temperature is shown in Table 1. With the increasing of ZrO_2 content, both monoclinic and cubic ZrO_2 phase increases. With the increasing of sintering temperature, a part of monoclinic ZrO_2 phase transformed into cubic phase, into which the co-added transition metal-oxides such as Sb, Cr, Mn and Co can be dissolved [33].

Fig. 2 shows the SEM microstructure of the prepared samples. The ZrO_2 content ranges from 0mol% to 2.0mol%, and the specimens were sintered between 1050°C to 1250°C. As shown in the figure, the microstructure of the ZnO varistor consists of the ZnO grains, the grain boundary layers and small particles located at the grain junctions. The ZnO grain size d decreases with ZrO_2 content and increases with sintering temperature. According to previous studies [13], [15], [19], [20], ZnO grains are mainly composed of ZnO crystals, and the grain boundary layers are mainly composed of Bi_2O_3, which acts as solvent and can dissolve the extrinsic elements. Excessive Bi_2O_3 can also promote the formation of spinal phases(Sb, Cr, Co, Mn). The spinal phases and ZrO_2 particles located at grain junctions can restrain the growth of ZnO grains.

In order to analyze the element composition of the prepared ZnO varistors, ZnO resistors with a ZrO_2 content of 2.0mol% and a sintering temperature of 1150°C were selected as samples for EDS analysis. The element distribution at each test point is shown in Table 2, it can be seen that, little Zr can be detected in test point 1 (spinel) and test point 2 (ZnO grain), while the content of Zr in point 3(ZrO_2 particle) increases significantly.

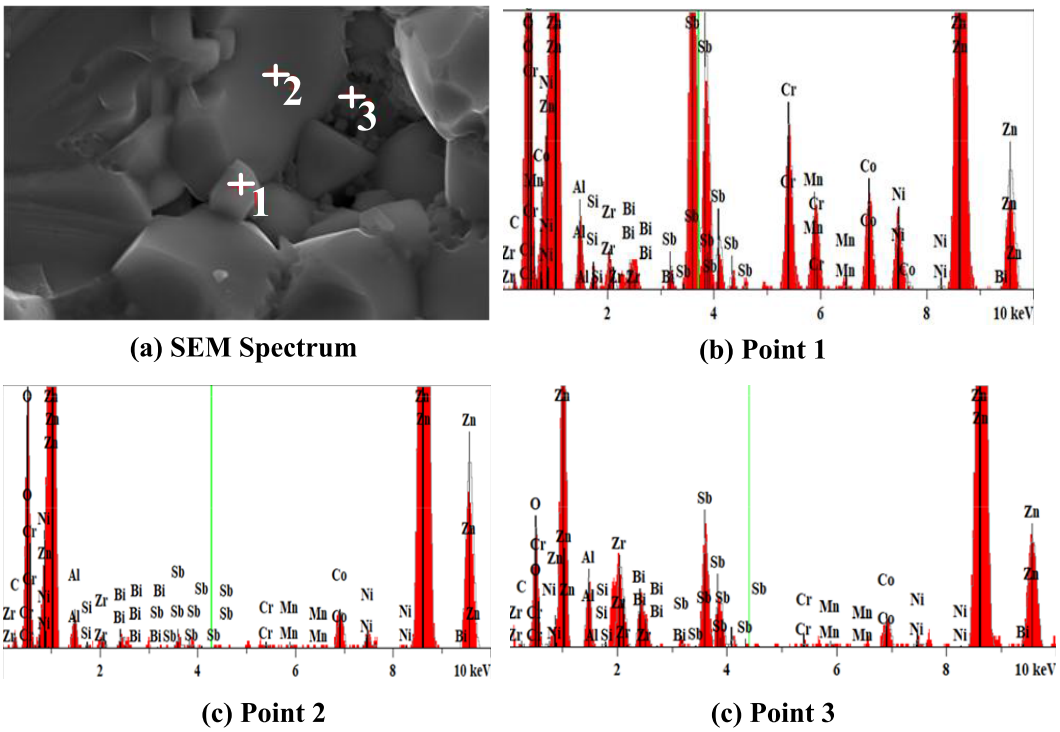

FIGURE 3. EDS pattern of the sample with 2mol% ZrO2 content and 1150°C sintering temperature.

TABLE 2. The element contents at different locations of ZnO resistance.

Position	Zn	Zr	Sb	Mn	Co	Cr
Point 1	59.2%	0.7%	11.2%	1.7%	2.9%	3.4%
Point 2	89.6%	0.4%	0.6%	0.2%	1.2%	0.2%
Point 3	81.1%	3.3%	1.6%	0.3%	1.4%	0.3%

Fig. 4 shows the variation of extinct element content (Sb, Cr, Co, Mn) with ZrO_2 content and sintering temperature obtained by EDS analysis. It can be seen that, in ZnO grains, ZrO_2 additive and sintering temperature affect little on the extinct element content. In grain boundary layers, when additive ZrO_2 content is less than 1.0mol%, the content of extrinsic elements increases slightly with ZrO_2 content. When ZrO_2 content is more than 1.0mol%, the content of extrinsic elements in the grain boundary layers decreases. This phenomenon is mainly because that, when ZrO_2 content is less than 1.0mol%, the increasing of ZrO_2 content can restrain the growth of ZnO grains and promote the formation of the grain boundaries, leading to more extrinsic elements dissolving into grain boundaries [15]. When ZrO_2 content continues to increase, as shown in Table 1, excessive grain boundaries and cubic phase ZrO_2 are generated, as cubic phase ZrO_2 can dissolve extrinsic elements, the concentration of extrinsic elements content in grain boundary layers decreases.

In order to explain the variation of extrinsic elements with sintering temperature in Fig.4, the formula of evaporation enthalpies of composites is introduced and expressed as below [11]–[13], [15], [19] :

$$HVAP_1 = 1.093RT_1[(\frac{T_1}{TC})(\frac{InPC - 1.013}{0.930 - T_1/TC})] \quad (2)$$

where R is constant, T_1 is sintering temperature, PC is the critical pressure and TC is the boiling point of composites. From the equation above, it can be seen that, when sintering temperature is lower than 1150°C, the temperature is below the boiling point of Bi_2O_3, the extrinsic element content in grain boundary layers changes little. When sintering temperature is higher than 1200°C (boiling point of Bi_2O_3), the volatilization effects of extrinsic elements become obvious [18], leading to the decreasing of extrinsic elements in grain boundary layers.

B. DENSIFICATION AND GRAIN GROWTH

The influence of ZrO_2 content and sintering temperature on the average grain size of ZnO varistors was obtained by linear intercept method [14], [17], which can be expressed as follow: draw a straight line in the microscope, count the number of grains intercepted in the straight line, then the average grain size can be obtained as $d = L/M$, in which L is the length of the straight liner and M is the ZnO grain number.

As shown in Fig. 5, it is confirmed that, the ZrO_2 exists as independent second phase and can restrain the growth of ZnO grains, under the same sintering temperature, the ZnO grain size decreases with ZrO_2 content. The growth of ZnO grains is decided by the diffusion of atoms in ZnO varistors,

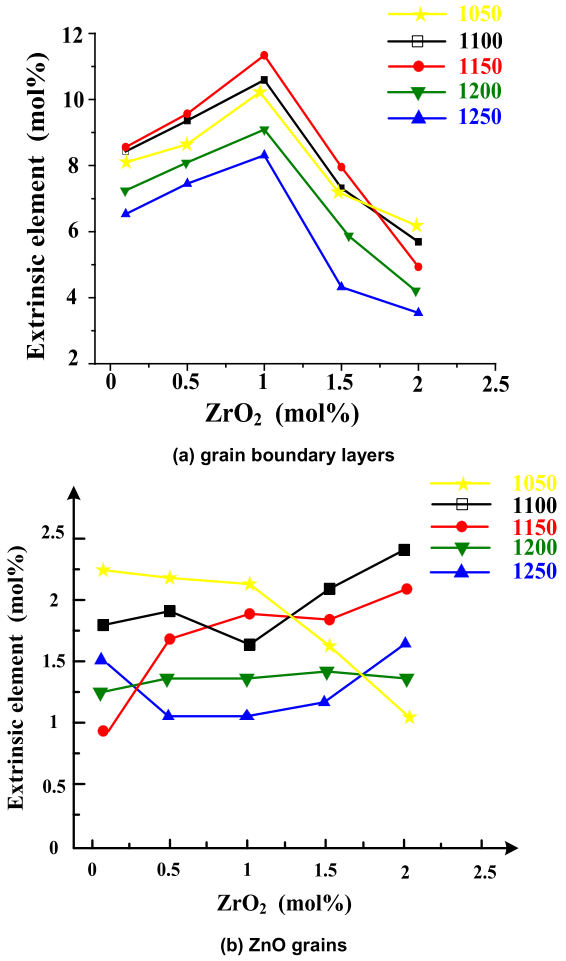

FIGURE 4. Extinct element variation with ZrO2 content and sintering temperature.

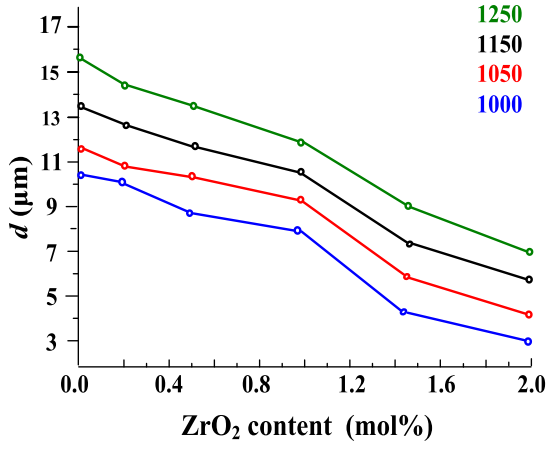

FIGURE 5. Influence of ZrO_2 dopants and sintering temperature on average grain size.

as sintering temperature become higher, the atomic diffusion velocity and ZnO grain size increases [4]–[10]. Bulk density can greatly affect the energy capacity of ZnO varistors, the influence of sintering temperature and ZrO_2 content on

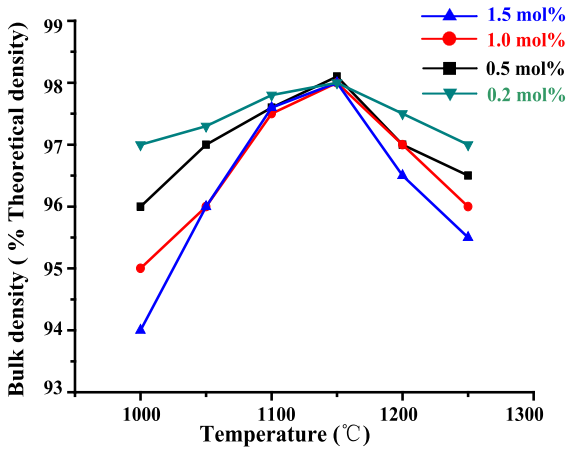

FIGURE 6. Influence of sintering temperature and ZrO_2 additive on the bulk density of ZnO varistors.

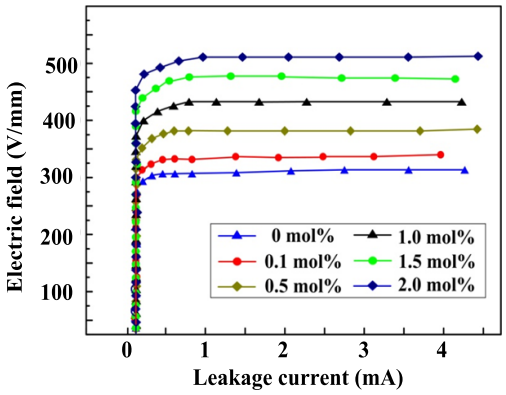

FIGURE 7. Influence of ZrO_2 content on the V-I characteristics with the sintering temperature of 1150°C.

the bulk density is shown in Fig.6, when sintering temperature is lower than 1100°C, the density of the sample increases with sintering temperature, and finally reach the max value (98% of the theoretical density, 5.67g/cm^3). When sintering temperature is lower than 1100°C or higher than 1200°C, bulk density of ZnO varistors with more than 1.0mol% ZrO_2 tend to decrease obviously. It is because that, when sintering temperature is lower than 1100°C, the growth of ZnO grains is incomplete, and the micropores in the green-pressing varistors are unfilled. When sintering temperature is higher than 1200°C, the volatilization effects become obvious and excessive micropores are also generated [18]. As ZrO_2 can restrain the growth of ZnO grains, when ZrO_2 content is more than 1.0mol%, the generation of micropores are promoted, leading to the decreasing of bulk density.

C. ELECTRIC CHARACTERISTICS

The V-I curve of the manufactured varistors sintered at 1150°C is shown in Fig.7, when ZrO_2 content is 0 mol%, the breakdown voltage is 305V/mm and when the ZrO_2 content increases to 2mol%, E_{1mA} increases to 510V/mm. The influence of ZrO_2 content and sintering temperature on the

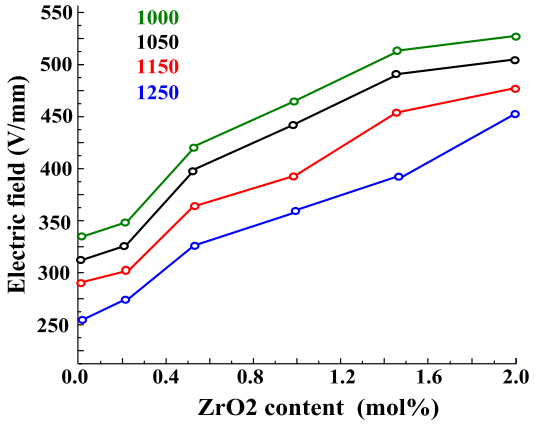

FIGURE 8. Voltage gradient variation with sintering temperature and ZrO2 contents.

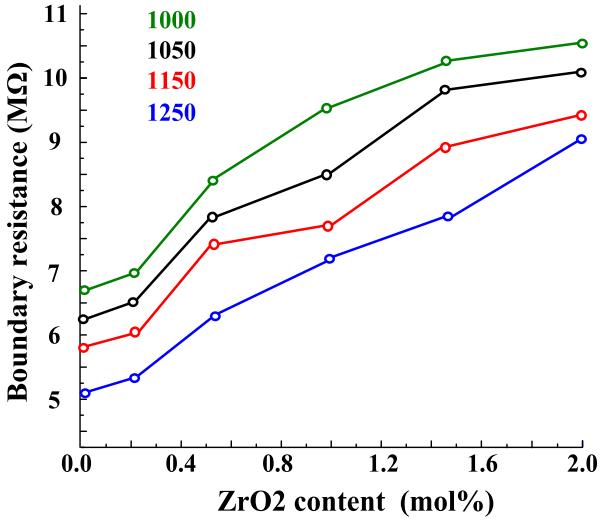

FIGURE 9. Variation of boundary layer resistance with sintering temperature and ZrO_2 contents.

breakdown voltage (E_{1mA}) is shown in Fig.8, from which it can be seen that, E_{1mA} increases with ZrO_2 content and decreases with sintering temperature.

Impedance analysis has been done to obtain the resistance of ZnO grain and grain boundary. The ZnO grain resistance remains 0.5Ω. As grain boundary resistance is much larger than that of ZnO grain, E_{1mA} is mainly dependent on ZnO grain boundary resistance. The variation of grain boundary resistance with ZrO_2 content and sintering temperature is shown Fig. 9. As shown in the figure, the grain boundary resistance is in proportion with E_{1mA}, which increases with ZrO_2 content and decreases with sintering temperature.

For the sintered ZnO varistors, the whole grain boundary resistance is decided by the average resistance per grain boundary ρ and the grain boundary number N. As the ZrO_2 particles can restrain the ZnO grain size while higher sintering temperature can promote the ZnO grain growth, N decreases with sintering temperature and increases with ZrO_2 content.

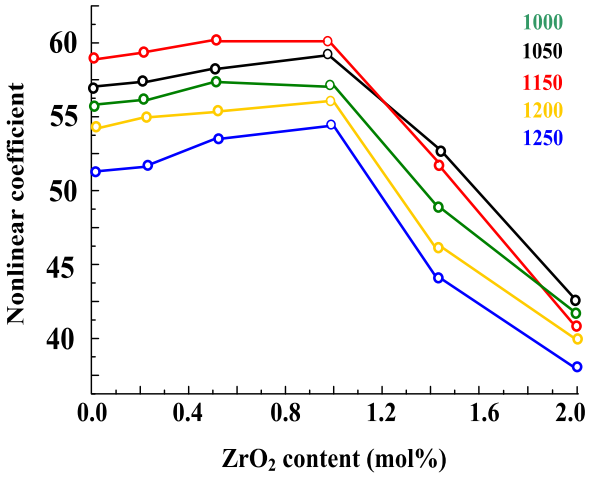

FIGURE 10. Influence of sintering temperature and ZrO_2 contents on the non-linear coefficient.

The average resistance per grain boundary ρ can be expressed as Equation (3) [22]–[24].

$$\rho = \rho_0 T \exp(-\frac{KT}{Q}) \tag{3}$$

In Equation (3), T means temperature, ρ_0 and K are constants. Q is the activation energy, Q increases with the barrier height Φ_B, which can be expressed in Equation (4) [12].

$$\Phi_B = \frac{e^2 N_S^2}{2\varepsilon_r \varepsilon_0 N_d} \tag{4}$$

In Equation (4), Ns is the interface states density, N_d is the donor density, ε_r, ε_0 and e are constants. It is confirmed that the extrinsic elements (Mn, Co, Sb and Cr) incorporated into ZnO grains can raise N_d, when dissolved into grain boundary layers, these extrinsic elements can increase Ns. From Fig. 4 and Fig. 5, it can be seen that, The change of Φ_B is not as obvious as grain boundary number N. Thus, as shown in Fig.7 and Fig.8, E_{1mA} increases with ZrO_2 content and decreases with sintering temperature.

Fig. 10 shows the influence of sintering temperature and additive ZrO_2 content on the nonlinear coefficient α of the manufactured varistors. For the sintering temperature of 1150°C, when the ZrO_2 content increases from 0 mol% to 1.0 mol%, α increases slightly from 56 to 58. As ZrO_2 content increases to 2.0 mol%, α decreases sharply to 43. When the sintering temperature increases from 1000°C to 1150°C, the nonlinear coefficients are very close to each other. However, as sintering temperature rises to 1250°C, α begins to decrease. α reaches to the highest value 58 when sintering temperature is 1150°C and ZrO_2 content is 1.0mol%.

The variation of leakage current (I_L) is shown in Fig. 11. With the increasing of ZrO_2 content, I_L tends to decrease first and then increase. When the sintering temperature is 1150°C or lower, the leakage currents are very close to each other, when sintering temperature continues to increase, I_L become obviously larger. When sintering temperature is

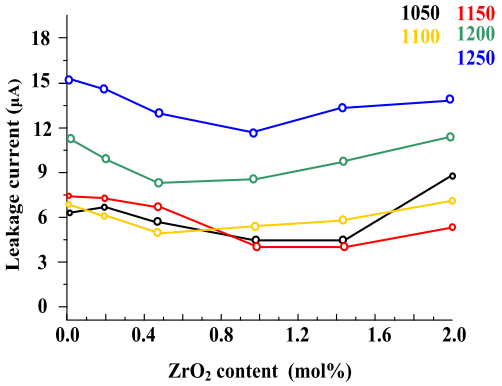

FIGURE 11. Influence of sintering temperature and additive ZrO2 contents on the leakage current.

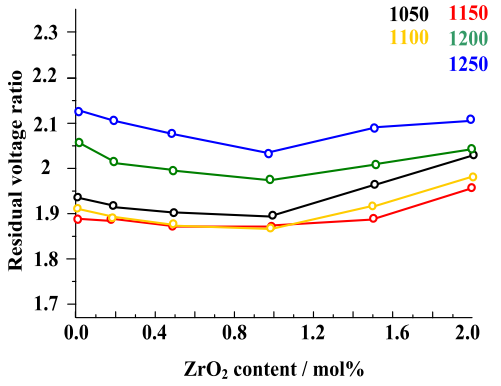

FIGURE 12. Influence of sintering temperature and additive ZrO2 contents on the residual voltage ratio.

1150°C and ZrO_2 content is 1.0mol%, I_L reaches the smallest value 4μA.

The variation of α and I_L can be explained by Equation (5) and Equation (6), in which J_0, β, K are constants, E means electric filed strength, T means temperature and J_L is the leakage current density [12]–[15].

$$\alpha = \frac{\gamma \Phi_B^{3/2}}{E} \tag{5}$$

$$J_L = J_0 \exp(-\frac{\Phi_B - \beta E^{1/2}}{KT}) \tag{6}$$

From Equation (5) and Equation (6), it can be known that, α and I_L are mainly decided by barrier height Φ_B. When ZrO_2 content is less than 1.0mol%, the increasing of ZrO_2 content can restrain ZnO grain size and promote the formation of grain boundary layers. Which causes more extrinsic elements dissolved into grain boundary layers, leading to higher Φ_B, higher α and lower J_L. When ZrO_2 content is more than 1.0 mol%, more ZrO_2 particles, especially cubic phase ZrO_2 are formed, leading to more extrinsic elements incorporated into ZrO_2 particles and less dissolved into the grain boundary layers, causing α lower and J_L higher. When sintering temperature is 1250°C or higher, more cubic phase ZrO_2 are generated, and volatilization effects of the metal oxide addictives such as Bi_2O_3 and Sb_2O_3 become much more serious, leading to less extrinsic elements dissolved into grain boundary layers. This may be the reason of the variation of α and I_L.

Applying 5kA, 4/10μs impulse current to the test samples, the variation of residual ratio (C_R) of the ZnO varitors can be obtained. As shown in Fig. 12, before 1.0mol%, the additive ZrO_2 has little influence on C_R, as ZrO_2 content continues to increase, C_R tends to increase. With the increasing of sintering temperature, C_R tends to decrease first and then increases. C_R researches its lowest value when ZrO_2 content is 1.0mol% and sintering temperature is 1150°C. This is mainly because that, when ZrO_2 content is 1.0mol% and sintering temperature is between 1100°C and 1200°C, the bulk density of these ZnO varistors reaches the highest value. The micro-structures of these varistors have better uniformities and fewer micropores, leading to the smallest C_R. As residual voltage ratio and bulk density are regarded as important parameters of surge handling ability, it can be confirmed that ZnO varistors with a sintering temperature of 1150°C and a ZrO_2 content of 1.0mol% can reach the optimum electric characteristics.

IV. CONCLUSION

In this paper, the effects of sintering temperature and ZrO_2 content on the micro-structure and electric characteristics have been investigated, XRD spectrum shows that the additive ZrO_2 exists as independent second phase in the ZnO varistors, with the increasing of sintering temperature, a part of monoclinic phase ZrO2 transforms to cubic phase, which can dissolve extrinsic elements such as Sb, Mn, Cr and Co. From the EDS analysis, with the increasing of ZrO_2, the content of extrinsic elements in the boundary layers increases first and then tends to decreases. The additive ZrO_2 can restrain the growth of ZnO grains and improve the voltage gradient of ZnO varistors, and the increasing of sintering temperature can promote the growth of ZnO grains, leading to the densification of ZnO varistors. When sintering temperature is 1250°C or higher, the volatilization of Bi_2O_3 and Sb_2O_3 become obvious, leading to the generation of excessive mocropores and degradation of electric characteristics. According to the experimental results, ZnO varistors sintered at 1150°C with 1.0mol% ZrO_2 can reach the overall optimum electric performance, exhibiting a leakage current of 4μA, a breakdown voltage of 420V/mm, a nonlinear coefficient of 58, and a residual voltage ratio of 1.87.

REFERENCES

[1] S. Gu, S. Wan, J. Wang, J. Chen, and T. Li, "Development and application of ±500 kV DC transmission line arrester in China power grid," *IEEE Trans. Power Del.*, vol. 33, no. 1, pp. 209–217, Jan. 2018.

[2] F. Kharchouche and S. Belkhiat, "Effect of spark plasma sintering on microstructure and electrical properties of ZnO-based varistors," *J. Mater. Sci., Mater. Electron.*, vol. 29, no. 19, pp. 16238–16247, 2018.

[3] F. Kharchouche and S. Belkhiat, "Effect of sintering temperature on microstructure and electrical properties of ZnO-0.5 mol%V_2O_5-0.5 mol%Cr_2O_3 varistors," *J. Mater. Sci., Mater. Electron.*, vol. 29, no. 5, pp. 3891–3897, 2018.

[4] F. Kharchouche and S. Belkhiat, "The effect of Sb_2O_3 content on the microstructure and electrical properties of (Mn_2O_3, V_2O_3)/ZnO varistor materials," in *Proc. 3rd Int. Conf. Elect. Sci. Technol. Maghreb (Cistem)*, Oct. 2018, pp. 1–5.

[5] S. Gu, W. Chen, J. He, H. Shen, and S. Zhang, "Development of surge arresters with series gap against lightning breakage of covered conductors on distribution lines," *IEEE Trans. Power Del.*, vol. 22, no. 4, pp. 2191–2198, Oct. 2007.

[6] R. Zeng, C. Zhuang, X. Zhou, S. Chen, Z. Wang, Z. Yu, and J. He, "Survey of recent progress on lightning and lightning protection research," *High Voltage*, vol. 1, no. 1, pp. 2–10, 2016.

[7] W. G. Carlson and T. K. Gupta, "Improved varistor nonlinearity via donor impurity doping," *J. Appl. Phys.*, vol. 53, no. 3, pp. 5746–5753, 1982.

[8] J. Fan and R. Freer, "The roles played by Ag and Al dopants in controlling the electrical properties of ZnO varistors," *J. Appl. Phys.*, vol. 77, no. 9, pp. 4795–4800, 1995.

[9] J. Han, P. Q. Mantas, and A. M. R. Senos, "Effect of Al and Mn doping on the electrical conductivity of ZnO," *J. Eur. Ceram. Soc.*, vol. 43, nos. 10–11, pp. 1883–1886, 2001.

[10] F. Kharchouche, S. Belkhiat, and D. Belkhiat, "Non-linear coefficient of $BaTiO_3$-doped ZnO varistor," *IET Sci., Meas. Technol.*, vol. 7, no. 6, pp. 326–333, 2013.

[11] D. Szwagierczak, J. Kulawik, and A. Skwarek, "Influence of processing on microstructure and electrical characteristics of multilayer varistors," *J. Adv. Ceram.*, vol. 8, no. 3, pp. 408–417, 2019.

[12] J.-J. Tian, H. Tian, Y.-H. Xu, Y.-J. Feng, and H.-L. He, "Nonlinear electrical properties and dielectric properties of ZnO ceramics doped with K_2CO_3," *J. Mater. Sci., Mater. Electron.*, vol. 30, no. 14, pp. 13768–13773, 2019.

[13] T. K. Roy, T. K. Bhattacharyya, and S. K. Thakur, "Role of sintering temperature on microstructure and nonlinear electrical properties of 0.1 mol.% Nb_2O_5 added ZnO–V_2O_5 varistor ceramics," *J. Mater. Sci., Mater. Electron.*, vol. 30, no. 6, pp. 5650–5661, 2019.

[14] D. Xu, K. He, B. H. Chen, S. Y. Mu, W. H. Wu, L. Jiao, X. J. Sun, and Y. T. Yang, "Effects of Cr_2O_3 doping on the microstructural and electrical properties of ZnO–Bi_2O_3 based varistor films," *J. Mater. Sci., Mater. Electron.*, vol. 26, no. 10, pp. 7909–7913, 2015.

[15] T. Takada and Y. Takada, "Correlation between electrical properties and crystalline phases for ZnO-Bi_2O_3 based varistor ceramics with rare earth additives," *J. Electroceram.*, vol. 31, nos. 1–2, pp. 138–142, 2013.

[16] S. Ezhilvalavan and T. R. N. Kutty, "Kutty dependence of non-linearity coefficients on transition metal oxide concentration in simplified compositions of ZnO+Bi_2O_3+MO varistor ceramics (M=Co or Mn)," *J. Mater. Sci., Mater. Electron.*, vol. 7, no. 12, pp. 137–148, 1996.

[17] F. Kharchouche and S. Belkhiat, "The effect of $BaTiO_3$ content on the microstructure and electrical properties of Bi_2O_3/ZnO varistor materials," in *Proc. 3rd Int. Conf. Elect. Sci. Technol. Maghreb*, Oct. 2018, pp. 1–6.

[18] F. Kharchouche, "Effect of sintering temperature on microstructure and electrical properties of ZnO-0.5 mol%V_2O_5-0.5 mol% Cr_2O_3 varistors," *J. Mater. Sci., Mater. Electron.*, vol. 29, no. 5, pp. 3891–3897, 2018.

[19] D. Xu, K. He, B. H. Chen, S. Y. Mu, W. H. Wu, L. Jiao, X. J. Sun, and Y. T. Yang, "Effects of Cr_2O_3 doping on the microstructural and electrical properties of ZnO-Bi_2O_3 based varistor films," *J. Mater. Sci., Mater. Electron.*, vol. 26, no. 10, pp. 7909–7913, 2015.

[20] S. Ezhilvalavan and T. R. N. Kutty, "Dependence of non-linearity coefficients on transition metal oxide concentration in simplified compositions of ZnO+Bi_2O_3+MO varistor ceramics (M=Co or Mn)," *J. Mater. Sci., Mater. Electron.*, vol. 7, no. 2, pp. 137–148, 1996.

[21] Z. Peng, X. Fu, Y. Zang, Z. Fu, C. Wang, L. Qi, and H. Miao, "Influence of Fe_2O_3 doping on microstructural and electrical properties of ZnO–Pr_6O_{11} based varistor ceramic materials," *J. Alloys Compounds*, vol. 508, no. 2, pp. 494–499, 2010.

[22] X. Su, Y. Jia, X. Liu, J. Wang, J. Xu, X. He, C. Fu, and S. Liu, "Preparation, dielectric property and infrared emissivity of Fe-doped ZnO powder by coprecipitation method at various reaction time," *Ceram. Int.*, vol. 40, no. 4, pp. 5307–5311, 2014.

[23] M. L. Dinesha, H. S. Jayanna, S. Ashoka, and G. T. Chandrappa, "Temperature dependent electrical conductivity of Fe doped ZnO nanoparticles prepared by solution combustion method," *J. Alloys Compounds*, vol. 485, nos. 1–2, pp. 538–541, 2009.

[24] Z. Lu, Y. Cai, Z. Chen, and J. Wu, "Effects of Fe impurity on performances of ZnO varistors," *Rare Metal Mater. Eng.*, vol. 36, no. 1, pp. 187–190, 2007.

[25] P. R. Bueno, E. R. Leite, M. M. Oliveira, M. O. Orlandi, and E. Longo, "Role of oxygen at the grain boundary of metal oxide varistors: A potential barrier formation mechanism," *Appl. Phys. Lett.*, vol. 79, no. 3, pp. 48–50, 2001.

[26] F. Stucki and F. Greuter, "Key role of oxygen at zinc oxide varistor grain boundaries," *Appl. Phys. Lett.*, vol. 57, no. 5, pp. 446–448, 1990.

[27] R. Merkle and J. Maier, "How is oxygen incorporated into oxides? A comprehensive kinetic study of a simple solid-state reaction with $SrTiO_3$ as a model material," *Angew. Chem. Int. Ed.*, vol. 47, no. 3, pp. 3874–3894, 2008.

[28] Z. H. Wu, J. H. Fang, D. Xu, Q.-D. Zhong, and L.-Y. Shi, "Effect of SiO_2 addition on the microstructure and electrical properties of ZnO-based varistors," *Int. J. Minerals Metall. Mater.*, vol. 17, no. 2, pp. 86–91, 2010.

[29] P. Meng, S. Gu, J. Wang, J. Hu, and J. He, "Improving electrical properties of multiple dopant ZnO varistor by doping with indium and gallium," *Ceram. Int.*, vol. 44, no. 1, pp. 1168–1171, 2018.

[30] C. W. Nahm, B.-C. Shin, and B.-H. Min, "Microstructure and electrical properties of Y_2O_3-doped ZnO–Pr_6O_{11}-based varistor ceramics," *Mater. Chem. Phys.*, vol. 82, no. 1, pp. 157–164, 2003.

[31] P. Li, Q. Liao, S. Yang, X. Bai, Y. Huang, X. Yan, Z. Zhang, S. Liu, P. Lin, Z. Kang, and Y. Zhang, "*In situ* transmission electron microscopy investigation on fatigue behavior of single ZnO wires under high-cycle strain," *Nano Lett.*, vol. 14, no. 2, pp. 480–485, 2014.

[32] M. Bartkowiak, M. G. Comber, and G. D. Mahan, "Failure modes and energy absorption capability of ZnO varistors," *IEEE Trans. Power Del.*, vol. 14, no. 3, pp. 152–162, Jan. 1999.

[33] C. H. Kim and J. H. Kim, "Microstructure and electrical properties of ZnO–ZrO_2–Bi_2O_3–M_3O_4 (MCo, Mn) varistors," *J. Eur. Ceram. Soc.*, vol. 24, no. 3, pp. 2537–2546, 2004.

[34] J. Kegel, F. Laffir, I. M. Povey, and M. E. Pemble, "Defect-promoted photo-electrochemical performance enhancement of orange-luminescent ZnO nanorod-arrays," *Phys. Chem. Chem. Phys.*, vol. 19, no. 9, pp. 12255–12268, 2017.

[35] G. Zhang, Q. Liao, M. Ma, F. Gao, Z. Zhang, Z. Kang, and Y. Zhang, "Uniformly assembled vanadium doped ZnO microflowers/bacterial cellulose hybrid paper for flexible piezoelectric nanogenerators and self-powered sensors," *Nano Energy*, vol. 52, no. 3, pp. 501–509, 2018.

[36] J. Han, A. M. R. Senors, and P. Q. Mantas, "Varistor behaviour of Mn-doped ZnO ceramics," *J. Eur. Ceram. Soc.*, vol. 22, pp. 1653–1660, Sep. 2002.

[37] Q. Fu, T. Chen, X. Ye, P. Chen, Y. Liu, C. Gao, Y. Hu, Z. Zheng, and D. Zhou, "ZnO varistor ceramics prepared by the reduction–reoxidation method," *J. Eur. Ceram. Soc.*, vol. 35, no. 2, pp. 3025–3031, 2015.

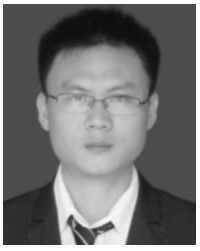

PENGKANG XIE was born in Hunan, China, in 1988. He received the Ph.D. degree in electrical engineering from Zhejiang University, Hangzhou, China, in 2016. He is currently with State Grid Corporation of China. His current research interests include external insulation, disaster prevention, and reduction of power systems.

JIANPING HU was born in Jiangxi, China, in 1987. He received the bachelor's and master's degrees in high-voltage engineering from Wuhan University. He is currently with the State Key Laboratory of Disaster Prevention and Reduction for Power Grid Transmission and Distribution Equipment.